Biosci. Rep. (2013) / **33** / art:e00014 / doi 10.1042/BSR20120069

Original Paper

OPEN ACCESS

Identification of the kinetic mechanism of succinyl-CoA synthetase

Xin LI, Fan WU and Daniel A. BEARD[1]

Biotechnology and Bioengineering Center and Department of Physiology, Medical College of Wisconsin, Milwaukee, WI 53216, U.S.A.

Synopsis

The kinetic mechanism of SCS [succinyl-CoA (coenzyme A) synthetase], which participates in the TCA (tricarboxylic acid) cycle, ketone body metabolism and haem biosynthesis, has not been fully characterized. Namely, a representative catalytic mechanism and associated kinetic parameters that can explain data on the enzyme-catalysed reaction kinetics have not been established. To determine an accurate model, a set of putative mechanisms of SCS, proposed by previous researchers, were tested against experimental data (from previous publication) on SCS derived from porcine myocardium. Based on comparisons between model simulation and the experimental data, an ordered ter–ter mechanism with dead-end product inhibition of succinate against succinyl-CoA is determined to be the best candidate mechanism. A thermodynamically constrained set of parameter values is identified for this candidate mechanism.

Key words: catalytic mechanism, dead-end binding, enzyme, succinyl-CoA.

Cite this article as: Li, X., Wu, F. and Beard, D.A. (2013) Identification of the kinetic mechanism of succinyl-CoA synthetase. Biosci. Rep. **33**(1), art:e00014.doi:10.1042/BSR20120069

INTRODUCTION

The substrate-level phosphorylation of nucleoside diphosphate catalysed by SCS (succinyl-CoA synthetase) is the only reaction in the TCA (tricarboxylic acid) cycle that is near reversible under physiological conditions [1]. In addition to its role in the TCA cycle, the SCS reaction is a part of ketone body metabolism [2] and haem biosynthesis [3] pathways. Abnormal SCS activities are associated with diabetes and neurodegenerative diseases [4–6].

Several competing models for the catalytic mechanism of SCS have been proposed based on kinetic studies. Kaufman [7] proposed that an enzyme-bound phosphoryl derivative of CoA serves as an intermediate in the mechanism (Figure 1A) based on exchange experiments performed with the spinach enzyme. In this mechanism, orthophosphate stimulates the exchange of succinate with succinyl-CoA and CoA inhibits the exchange of ADP with ATP [7]. Later, Cleland proposed a partially random mechanism with dead-end complexes (Figure 1B) to fit the data reported by Cha and Parks [8] who used azaGDP and azaGTP as substitutes for GDP and GTP in some of the initial velocity studies. Four main conclusions were drawn from these studies. First, at least one product was released from the enzyme between the time of addition of the two substrates, phosphate and azaGDP/succinyl-CoA in the CoA formation reaction. Secondly, no product was released between the addition of azaGDP and succinyl-CoA in the CoA formation reaction. Thirdly, no product was released between the addition of CoA and azaGTP in the succinyl-CoA formation reaction. Finally, for the succinyl-CoA formation reaction, succinate bound to the enzyme after a product was released with its low concentrations, but before a product was released with its sufficiently high concentrations. Cha et al. [9] and Moyer et al. [10] proposed a Hexa-Uni Ping Pong ter–ter mechanism with enzyme-bound CoA as a high-energy intermediate (Figure 1C) according to their finding that the exchange of GDP with GTP only required Mg^{2+} and the exchange of phosphate and GTP required CoA and Mg^{2+}. Hager [11] proposed a mechanism similar to that of Kaufman [7] with a different releasing order for the products succinate and CoA (Figure 1D) based on the possibility of the existence of an undissociable enzyme-bound succinyl phosphate as an intermediate. Although Hager argued against the existence of this intermediate, Bridger [1] argued for it. Nishimura [12,13] reported direct evidence for the intermediate from experiments using *Escherichia coli* SCS. Kohn et al. [14] proposed a simple ordered ter–ter mechanism (Figure 1E) based on two assumptions: first, the concentrations of substrates always exceed their respective K_m values; second, the flux is primarily controlled by the deviation of the mass action ratio from the equilibrium constant. Finally, Moffet and Bridger [15,16] proposed a

Abbreviations used: AIC, Akaike information criterion; SCS, succinyl-CoA synthetase; TCA, tricarboxylic acid.

[1]To whom correspondence should be addressed (email beardda@gmail.com).

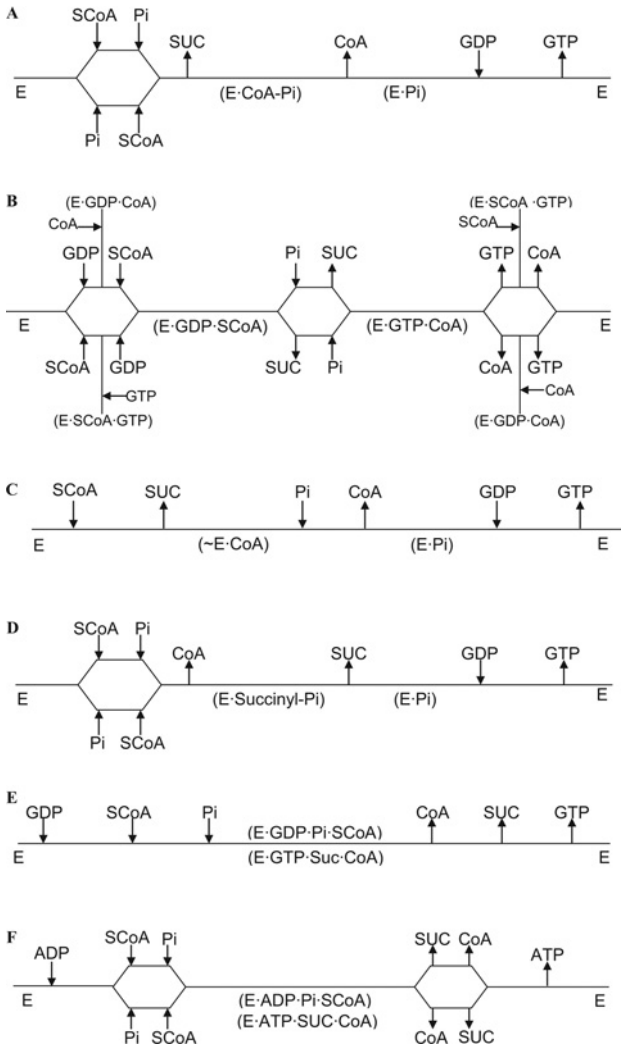

Figure 1 Kinetic steps of candidate models

(**A**) Mechanism proposed by Kaufman [7]: enzyme-bound phosphoryl derivative of CoA as an intermediate. (**B**) Mechanism proposed by Cleland [8]: a complicated fully random with dead-end complexes. (**C**) A Hexa-Uni Ping Pong ter–ter mechanism proposed by Cha et al. [9] and Moyer et al. [10]: high-energy enzyme-bound CoA as an intermediate. (**D**) Mechanism supported by Nishimura [12,13]: enzyme-bound succinyl phosphate as an intermediate. (**E**) Ordered ter–ter mechanism proposed by Kohn et al. [14]. (**F**) A partially random sequential kinetic mechanism proposed by Moffer and Bridger [15,16].

partially random sequential kinetic mechanism (Figure 1F) based on initial rate kinetic studies of *E. coli* SCS. In their studies, CoA and succinate appear to be kinetically equivalent in the succinyl-CoA formation reaction, analogous to succinyl-CoA and phosphate in the CoA formation reaction; succinyl-CoA should be released before ADP was released. However, they report that the ordered ter–ter mechanism was a reasonable approximation [16].

Although these studies point to several plausible catalytic mechanisms, controversial issues remain and no model has been shown to sufficiently explain all of the relevant data. In the present study, these catalytic mechanisms are used to build a set of mathematical models representing the mechanisms. Model simulations are compared with experimental data to eliminate candidate models and determine a consensus mechanism that best explains experimental observations.

EXPERIMENTAL

The strategy used in the present study is to use quasi-steady-state approximations to express reaction fluxes in terms of activities of chemical species, in which the effects of pH, ionic strength and cation binding to biochemical species are explicitly accounted for in the analysis of the data [17,18]. This strategy can maintain the relationship between the kinetic constants and the reaction equilibrium constant and will be useful to analyse kinetic data from other enzymes.

Reaction thermodynamics

SCS catalyses the reversible reaction:

$$\mathrm{GDP} + \mathrm{SCoA} + \mathrm{P_i} \leftrightarrow \mathrm{GTP} + \mathrm{SUC} + \mathrm{CoA} \quad (1)$$

a biochemical reaction in which each biochemical reactant represents a sum of rapidly interconverting chemical species. Abbreviations and associated species of each reactant are defined in Table 1. The corresponding reference chemical reaction is:

$$\mathrm{GDP^{3-}} + \mathrm{SCoA^{-}} + \mathrm{P_i^{2-}} \leftrightarrow \mathrm{GTP^{4-}} + \mathrm{SUC^{2-}} + \mathrm{CoA^{-}} + \mathrm{H^{+}} \quad (2)$$

where a superscript is used to indicate the charge of chemical species. The equilibrium constant is defined as:

$$K_{\mathrm{eq}} = \left(\frac{[\mathrm{CoA^{-}}][\mathrm{SUC^{2-}}][\mathrm{GTP^{4-}}][\mathrm{H^{+}}]}{[\mathrm{GDP^{3-}}][\mathrm{SCoA^{-}}][\mathrm{P_i^{2-}}]} \right)_{\mathrm{eq}} \quad (3)$$

The standard Gibbs free energy ($T = 298.15$ K, $I = 0$ M), computed via:

$$\Delta_{\mathrm{r}}G^{0} = \Delta_{\mathrm{f}}G^{0}_{\mathrm{CoA}} + \Delta_{\mathrm{f}}G^{0}_{\mathrm{SUC}} + \Delta_{\mathrm{f}}G^{0}_{\mathrm{GTP}} - \Delta_{\mathrm{f}}G^{0}_{\mathrm{GDP}} - \Delta_{\mathrm{f}}G^{0}_{\mathrm{SCoA}} - \Delta_{\mathrm{f}}G^{0}_{\mathrm{P_i}} = 56.55\,\mathrm{kJ/mol} \quad (4)$$

is related to the equilibrium constant K_{eq} via the standard relationship $\Delta_{\mathrm{r}}G^{0} = -RT \ln K_{\mathrm{eq}}$

Binding polynomials are used to account for the relationship between species and reactant concentrations. For example,

$$[\mathrm{CoA^{-}}] = [\mathrm{CoA}] / P_{\mathrm{CoA}} \quad (5)$$

where [CoA] is the total reactant concentration and P_{CoA} is the binding polynomial for CoA. The binding polynomial for reactant j is a function of the pH and free concentrations of metal cations [19]:

$$P_j = 1 + \frac{h}{K_{h1,j}} + \frac{h^2}{K_{h1,j}K_{h2,j}} + \frac{[\mathrm{Mg^{2+}}]}{K_{\mathrm{Mg1},j}} + \frac{h[\mathrm{Mg^{2+}}]}{K_{h1,j}K_{h\mathrm{Mg},j}} + \frac{[\mathrm{Mg^{2+}}]^2}{K_{\mathrm{Mg1},j}K_{\mathrm{Mg2},j}} + \cdots \quad (6)$$

Table 1 Thermodynamic parameter values for SCS (values computed for $T = 298.15$ K)
All of the values come from Li et al. [19].

Reactant	Abbreviation	Reference species	$\Delta_f G^0$ (kJ/mol) (at $I = 0$ M)	Ion-bound species	pK (at $I = 0.1$ M)
Co-enzyme A	CoA	CoA^-	− 57.17	$COASH^\circ$	8.17
Guanosine diphosphate	GDP	GDP^{3-}	− 1904.22	$HGDP^{2-}$	6.505
				H_2GDP^-	2.8
				$MgGDP^-$	3.4
Guanosine triphosphate	GTP	GTP^{4-}	− 2768.10	$HGTP^{3-}$	6.63
				H_2GTP^{2-}	2.93
				$MgGTP^{2-}$	4.31
				$MgHGTP^-$	2.31
Orthophosphate	P_i	P_i^{2-}	− 1096.10	HP_i^-	6.78
				$H_2P_i^0$	1.945
				MgP_i^0	1.823
				$MgHP_i^+$	0.669
				KP_i^-	0.5
Succinate	SUC	SUC^{2-}	− 589.56	$HSUC^-$	5.275
				H_2SUC^0	4.02
				$MgSUC^0$	1.355
				$MgHSUC^+$	0.62
				$KSUC^-$	0.43
Succinyl-CoA	SCoA	$SCoA^-$	− 471.06	$HSCOA^0$	3.99

where h is the hydrogen ion activity ($h = 10^{-pH}$), and the K values represent cation dissociation constants, obtained from Li et al. [19]. For the calculations used here, all values are corrected for the effects of temperature and ionic strength as detailed in Li et al. [20]. Thermodynamic data used in this study are listed in Table 1.

The activity, a, of a chemical species is defined as the product of an activity coefficient, γ, and species concentration, c: $a = \gamma \cdot c$. The activity coefficient γ is estimated from the extended Debye–Hückel equation [21,22]:

$$\ln \gamma = -\frac{\alpha(T) z^2 I^{1/2}}{1 + B I^{1/2}} \quad (7)$$

where I is the ionic strength in Molar (M) units, z is the valence of species, and B is an empirical constant taken to be 1.6 $M^{-1/2}$. The quantity $\alpha(T)$ is an empirical function that varies with temperature:

$$\alpha(T) = 1.10708 - (1.54508 \times 10^{-3})T + (5.95584 \times 10^{-6})T^2 \quad (8)$$

where T is in Kelvin (K) units.

Fundamental kinetic mechanisms

Studies found SCS is widely expressed in mouse, pigeon, pig and human tissues [23]. The percentage identities of β-chain sequences of mammalian SCS from mouse, pigeon and human tissues are at least 89%, and β-subunit of pig SCS has the highest identity ($\geqslant$94%) to human compared with mouse and pigeon [23]. Since the most complete available experimental data on SCS kinetics are associated with the enzyme derived from pig heart [8], we use this set of data to identify and evaluate the competing models. Six previously proposed putative mechanisms for SCS are illustrated in Figure 1. As mechanism F was proposed for *E. coli* SCS (which has a different structure from mammalian SCS [1,24]), and it is effectively approximated by mechanism E [15], we exclude it from our list of competing models. Therefore there are in total five mechanisms in our test list, as summarized in Table 2.

Derivation of quasi-steady-state models

Since the total amount of enzyme is much lower than the initial reactants concentration used in Cha and Parks' experiments [8], quasi-steady-state and quasi-equilibrium approximations are used to represent the kinetics of the enzyme-catalysed reaction. Expressions for rate equations, the Michaelis (K_m) and inhibition (K_i) constants of mechanism B, C and E have been provided by Cleland [8,25] and Segel [26]. Applying the methods of Cleland [25], the rate equations for mechanisms A and D are derived as detailed in the Appendix.

Model parameterization

As in Mescam et al. [18], an effective charge is assigned to each enzyme–substrate complex in order to account for the effects of ionic strength on the kinetics. (This is necessary because the ionic strength of the reaction media in the experiments of Cha and Parks ranges from 0.1122 to 0.2163 M, resulting in an estimated activity coefficient range of 0.7289–0.7721 for a monovalent species and 0.0063–0.0159 for a quadrivalent species such as GTP^{4-}.)

Table 2 A list of models and corresponding mechanisms

No.	Mechanism	Reference(s)
1	A: partial random sequential kinetic mechanism with enzyme-bound phosphoryl CoA as an intermediate	[7]
2	B: complicated fully random with dead-end complexes kinetic mechanism	[8]
3	C: hexa-Uni Ping Pong ter–ter mechanism with high-energy enzyme-bound CoA as an intermediate	[9,10]
4	D: partial random sequential kinetic mechanism with enzyme-bound succinyl phosphate as an intermediate	[12]
5	E: ordered ter–ter kinetic mechanism	[14]

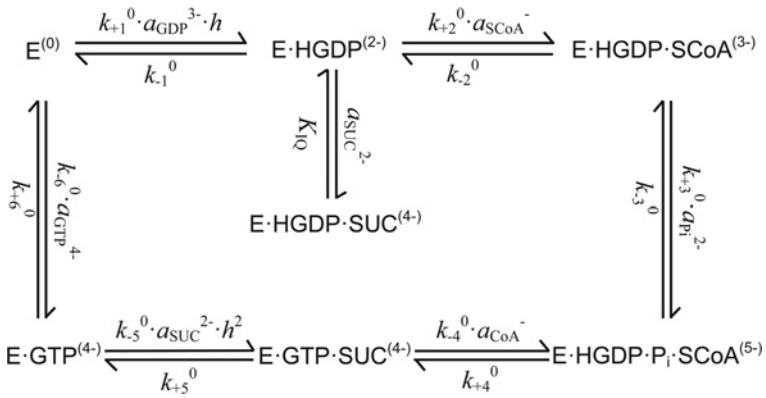

Figure 2 Ordered ter–ter mechanism with dead-end of succinate binding to enzyme state 2
k_i^0 is the rate constant at $T = 303.15$ K, a is the chemical activity variable for each chemical species, h is the hydrogen ion activity, and K_{IQ} is the dissociation constant of succinate from the dead-end complex $E \cdot HGDP \cdot SUC^{(4-)}$.

Assigned charges for the ordered ter–ter mechanism (mechanism E) with charged enzyme–substrate complex are shown in Figure 2, as an example. Since the experimental temperature and pH value was held constant at 303.15 K and 7.4 respectively in all of experiments to be analysed here [8,27], we can define:

$$k_{+1}^* = k_{+1}^0 h,\ k_{-5}^* = k_{-5}^0 h^2 \tag{9}$$

where k_i^0 is the rate constant at $T = 303.15$ K and h is the hydrogen ion activity. After assigning charges to each state, the individual rate constants take the form $k = \gamma_c k^0$, where γ is the activity coefficient with absolute value of charge c of the corresponding enzyme–substrate complex. For example, as shown in Figure 2, $E \cdot HGDP^{(2-)}$ has two negative charges, and it related to two rate constants k_{-1}^0 and k_{+2}^0 as the reactant, therefore $k_{-1} = \gamma_2 k_{-1}^0$ and $k_{+2} = \gamma_2 k_{+2}^0$. Thus, the rate constants are:

$$\begin{aligned}
&k_{+1} = k_{+1}^*,\ k_{-1} = \gamma_2 k_{-1}^0,\ k_{+2} = \gamma_2 k_{+2}^0,\ k_{-2} = \gamma_3 k_{-2}^0,\\
&k_{+3} = \gamma_3 k_{+3}^0,\ k_{-3} = \gamma_5 k_{-3}^0,\ k_{+4} = \gamma_5 k_{+4}^0,\ k_{-4} = \gamma_4 k_{-4}^0,\\
&k_{+5} = \gamma_4 k_{+5}^0,\ k_{-5} = \gamma_4 k_{-5}^*,\ k_{+6} = \gamma_4 k_{+6}^0,\ k_{-6} = k_{-6}^0
\end{aligned} \tag{10}$$

where the activity coefficients are calculated from eqn (7). Michaelis (K_m) and inhibition (K_i) constants, and maximum velocities (V_m) for this mechanism are computed as follows:

$$K_{mA} = \frac{k_{+4}k_{+5}k_{+6}}{k_{+1}(k_{+4}k_{+5} + k_{+4}k_{+6} + k_{+5}k_{+6})}$$

$$= \frac{\gamma_5 k_{+4}^0 \cdot \gamma_4 k_{+5}^0 \cdot \gamma_4 k_{+6}^0}{k_{+1}^0 h \cdot (\gamma_5 k_{+4}^0 \cdot \gamma_4 k_{+5}^0 + \gamma_5 k_{+4}^0 \cdot \gamma_4 k_{+6}^0 + \gamma_4^2 k_{+5}^0 k_{+6}^0)},$$

$$K_{mB} = \frac{k_{+4}k_{+5}k_{+6}}{k_{+2}(k_{+4}k_{+5} + k_{+4}k_{+6} + k_{+5}k_{+6})}$$

$$= \frac{\gamma_5 k_{+4}^0 \cdot \gamma_4 k_{+5}^0 \cdot \gamma_4 k_{+6}^0}{\gamma_2 k_{+2}^0 \cdot (\gamma_5 k_{+4}^0 \cdot \gamma_4 k_{+5}^0 + \gamma_5 k_{+4}^0 \cdot \gamma_4 k_{+6}^0 + \gamma_4^2 k_{+5}^0 k_{+6}^0)},$$

$$K_{mC} = \frac{k_{+5}k_{+6}(k_{-3} + k_{+4})}{k_{+3}(k_{+4}k_{+5} + k_{+4}k_{+6} + k_{+5}k_{+6})}$$

$$= \frac{\gamma_4 k_{+5}^0 \cdot \gamma_4 k_{+6}^0 \cdot (\gamma_5 k_{-3}^0 + \gamma_5 k_{+4}^0)}{\gamma_3 k_{+3}^0 \cdot (\gamma_5 k_{+4}^0 \cdot \gamma_4 k_{+5}^0 + \gamma_5 k_{+4}^0 \cdot \gamma_4 k_{+6}^0 + \gamma_4^2 k_{+5}^0 k_{+6}^0)},$$

$$K_{mP} = \frac{k_{-1}k_{-2}(k_{-3} + k_{+4})}{k_{-4}(k_{-1}k_{-2} + k_{-1}k_{-3} + k_{-2}k_{-3})}$$

$$= \frac{\gamma_2 k_{-1}^0 \cdot \gamma_3 k_{-2}^0 \cdot (\gamma_5 k_{-3}^0 + \gamma_5 k_{+4}^0)}{\gamma_4 k_{-4}^0 \cdot (\gamma_2 k_{-1}^0 \cdot \gamma_3 k_{-2}^0 + \gamma_2 k_{-1}^0 \cdot \gamma_5 k_{-3}^0 + \gamma_3 k_{-2}^0 \cdot \gamma_5 k_{-3}^0)},$$

$$K_{mQ} = \frac{k_{-1}k_{-2}k_{-3}}{k_{-5}(k_{-1}k_{-2} + k_{-1}k_{-3} + k_{-2}k_{-3})}$$

$$= \frac{\gamma_2 k_{-1}^0 \cdot \gamma_3 k_{-2}^0 \cdot \gamma_5 k_{-3}^0}{\gamma_4 k_{-5}^0 h^2 \cdot (\gamma_2 k_{-1}^0 \cdot \gamma_3 k_{-2}^0 + \gamma_2 k_{-1}^0 \cdot \gamma_5 k_{-3}^0 + \gamma_3 k_{-2}^0 \cdot \gamma_5 k_{-3}^0)},$$

$$K_{mR} = \frac{k_{-1}k_{-2}k_{-3}}{k_{-6}(k_{-1}k_{-2} + k_{-1}k_{-3} + k_{-2}k_{-3})}$$

$$= \frac{\gamma_2 k_{-1}^0 \cdot \gamma_3 k_{-2}^0 \cdot \gamma_5 k_{-3}^0}{k_{-6}^0 \cdot (\gamma_2 k_{-1}^0 \cdot \gamma_3 k_{-2}^0 + \gamma_2 k_{-1}^0 \cdot \gamma_5 k_{-3}^0 + \gamma_3 k_{-2}^0 \cdot \gamma_5 k_{-3}^0)},$$

$$K_{ia} = \frac{k_{-1}}{k_{+1}} = \frac{\gamma_2 k^0_{-1}}{k^0_{+1} h},\ K_{ib} = \frac{k_{-2}}{k_{+2}} = \frac{\gamma_3 k^0_{-2}}{\gamma_2 k^0_{+2}},$$

$$K_{ic} = \frac{k_{-3}}{k_{+3}} = \frac{\gamma_5 k^0_{-3}}{\gamma_3 k^0_{+3}},\ K_{ip} = \frac{k_{+4}}{k_{-4}} = \frac{\gamma_5 k^0_{+4}}{\gamma_4 k^0_{-4}},$$

$$K_{iq} = \frac{k_{+5}}{k_{-5}} = \frac{k^0_{+5}}{k^0_{-5} h^2},\ K_{ir} = \frac{k_{+6}}{k_{-6}} = \frac{\gamma_4 k^0_{+6}}{k^0_{-6}},$$

$$V_{mf} = [\mathrm{E}]_t \frac{k_{+4}k_{+5}k_{+6}}{k_{+4}k_{+5} + k_{+5}k_{+6} + k_{+4}k_{+6}},$$

$$V_{mr} = [\mathrm{E}]_t \frac{k_{-1}k_{-2}k_{-3}}{k_{-1}k_{-2} + k_{-2}k_{-3} + k_{-1}k_{-3}} \quad (11)$$

For the dead-end inhibition step shown in Figure 2, the dissociation constant is $K_{IQ} = \frac{[\mathrm{E}_2^{(2-)}][a_{\mathrm{SUC}^{2-}}]}{[\mathrm{E}_7^{(4-)}]}$

Substituting $\frac{[\mathrm{E}_1^{(0)}][a_{\mathrm{GDP}^{3-}}]}{[\mathrm{E}_2^{(2-)}]} = \frac{\gamma_2 k^0_{-1}}{k^0_{+1} h} = K_{ia}$, we have $[\mathrm{E}_7^{(4-)}] = \frac{[\mathrm{E}_2^{(2-)}][a_{\mathrm{SUC}^{2-}}]}{K_{IQ}} = \frac{[a_{\mathrm{GDP}^{3-}}][a_{\mathrm{SUC}^{2-}}]}{K_{ia}K_{IQ}}[\mathrm{E}_1^{(0)}]$.

Defining $\mathrm{A} = a_{\mathrm{GDP}^{3-}}$, $\mathrm{B} = a_{\mathrm{SCoA}^{-}}$, $\mathrm{C} = a_{\mathrm{P_i}^{2-}}$, $\mathrm{P} = a_{\mathrm{CoA}^{-}}$, $\mathrm{Q} = a_{\mathrm{SUC}^{2-}}$, and $\mathrm{R} = a_{\mathrm{GTP}^{4-}}$, and, the overall rate equation is:

$$\begin{aligned} v = \frac{V_{mf}V_{mr}(\mathrm{ABC} - \frac{\mathrm{PQR}}{K_{eq\_sim}})}{V_{mr}K_{ia}K_{ib}K_{mC}(1 + \mathrm{AQ}/K_{ia}/K_{IQ}) + V_{mr}K_{ib}K_{mC}\mathrm{A} + V_{mr}K_{ia}K_{mB}\mathrm{C}(1 + \mathrm{AQ}/K_{ia}/K_{IQ})} \\ + V_{mr}K_{mC}\mathrm{AB} + V_{mr}K_{mB}\mathrm{AC} + V_{mr}K_{mA}\mathrm{BC}(1 + \mathrm{AQ}/K_{ia}/K_{IQ}) + V_{mr}\mathrm{ABC} \\ + \frac{V_{mf}K_{ir}K_{mQ}\mathrm{P}}{K_{eq\_sim}}(1 + \mathrm{AQ}/K_{ia}/K_{IQ}) + \frac{V_{mf}K_{iq}K_{mP}\mathrm{R}}{K_{eq\_sim}} + \frac{V_{mf}K_{mR}\mathrm{PQ}}{K_{eq\_sim}}(1 + \mathrm{AQ}/K_{ia}/K_{IQ}) \\ + \frac{V_{mf}K_{mQ}\mathrm{PR}}{K_{eq\_sim}} + \frac{V_{mf}K_{mP}\mathrm{QR}}{K_{eq\_sim}} + \frac{V_{mf}\mathrm{PQR}}{K_{eq\_sim}} + \frac{V_{mf}K_{mQ}K_{ir}\mathrm{AP}}{K_{ia}K_{eq\_sim}} + \frac{V_{mr}K_{ia}K_{mB}\mathrm{CR}}{K_{ir}} \\ + \frac{V_{mf}K_{mQ}K_{ir}\mathrm{ABP}}{K_{ia}K_{ib}K_{eq\_sim}} + \frac{V_{mr}K_{mA}\mathrm{BCR}}{K_{ir}} + \frac{V_{mf}K_{mR}\mathrm{APQ}}{K_{ia}K_{eq\_sim}} + \frac{V_{mr}K_{ia}K_{mB}\mathrm{CQR}}{K_{iq}K_{ir}} \\ + \frac{V_{mf}K_{mQ}K_{ir}\mathrm{ABCP}}{K_{ia}K_{ib}K_{ic}K_{eq\_sim}} + \frac{V_{mf}K_{ip}K_{mR}\mathrm{ABCQ}}{K_{ia}K_{ib}K_{ir}K_{eq\_sim}} + \frac{V_{mf}K_{mR}\mathrm{ABPQ}}{K_{ia}K_{ib}K_{eq\_sim}} + \frac{V_{mr}K_{mA}\mathrm{BCQR}}{K_{iq}K_{ir}} \\ + \frac{V_{mr}K_{mA}K_{ic}\mathrm{BPQR}}{K_{ip}K_{iq}K_{ir}} + \frac{V_{mr}K_{ia}K_{mB}\mathrm{CPQR}}{K_{ip}K_{iq}K_{ir}} + \frac{V_{mf}K_{mR}\mathrm{ABCPQ}}{K_{ia}K_{ib}K_{ic}K_{eq\_sim}} + \frac{V_{mr}K_{mA}\mathrm{BCPQR}}{K_{ip}K_{iq}K_{ir}} \end{aligned} \quad (12)$$

where $K_{eq\_sim} = \frac{k_{+1}k_{+2}k_{+3}k_{+4}k_{+5}k_{+6}}{k_{-1}k_{-2}k_{-3}k_{-4}k_{-5}k_{-6}} = \frac{k^0_{+1}k^0_{+2}k^0_{+3}k^0_{+4}k^0_{+5}k^0_{+6}}{k^0_{-1}k^0_{-2}k^0_{-3}k^0_{-4}k^0_{-5}k^0_{-6}} \cdot \frac{1}{h}$.
Since the net production is equal to the net consumption in equilibrium, we can show that:

$$\begin{aligned} & k^0_{+1}a_{\mathrm{GDP}^{3-}}h \cdot k^0_{+2}a_{\mathrm{SCoA}^{-}} \cdot k^0_{+3}a_{\mathrm{Pi}^{2-}} \cdot k^0_{+4} \cdot k^0_{+5} \cdot k^0_{+6} \\ & = k^0_{-1} \cdot k^0_{-2} \cdot k^0_{-3} \cdot k^0_{-4}a_{\mathrm{CoA}^{-}} \cdot k^0_{-5}a_{\mathrm{SUC}^{-}}h^2 \cdot k^0_{-6}a_{\mathrm{GTP}^{4-}} \end{aligned} \quad (13)$$

Combining eqn (3) and (13) we obtain a definition of the constant $K_{\mathrm{eq\_sim}}$ in eqn (12):

$$K_{\mathrm{eq}} = \frac{k^0_{+1}k^0_{+2}k^0_{+3}k^0_{+4}k^0_{+5}k^0_{+6}}{k^0_{-1}k^0_{-2}k^0_{-3}k^0_{-4}k^0_{-5}k^0_{-6}} = K_{\mathrm{eq\_sim}} \cdot h \quad (14)$$

RESULTS

Ionic strength calculations

Data from Figures 5–12 of Cha and Parks [8] were compared with predictions from the five competing test models. For each data point, ionic strength was estimated based on estimating the free ion concentration of each species in the buffer on the basis of mass and charge balances [20]. Estimated ionic strength ranges are reported in the legends to Figures 3, 4 and 6.

Model fits to data

To estimate model parameters and evaluate the ability of candidate models to explain the data, an objective function was defined as the sum of normalized squared differences between model predictions of reaction flux and measured data:

$$M = \sum_{i\mathrm{Fig}=5}^{12} \sum_{i=1}^{\mathrm{FixReactant}} \frac{\sum_{j=1}^{\mathrm{VarReactant}} (J^{\mathrm{sim}}_{i,j} - J^{\mathrm{exp}}_{i,j})^2}{\sum_{j=1}^{n} (J^{\mathrm{exp}}_{i,j})^2} \quad (15)$$

where $J^{\mathrm{sim}}_{i,j}$ is the simulated flux and $J^{\mathrm{exp}}_{i,j}$ is the experimental flux. Model parameter estimates were obtained (using the fmincon function in MATLAB) by minimizing the sum-of-squared-errors objective function. Based on this analysis, mechanisms A and E were found to be able to match the majority of the data of Cha and Parks. (Corresponding simulation results for mechanisms B, C and D, which are not able to match the experimental observations simultaneously, are shown in the Appendix.)

Figure 3 illustrates model predictions based on mechanism A; Figure 4 illustrates predictions based on mechanism E. Although mechanisms A and E are able to match most of the experimental data, mechanism A is unable to reproduce the phosphate-dependent inhibition of the reverse reaction illustrated in Figure 3(F), where the dashed line is the case of $[\mathrm{P_i}]$ equal to zero, the solid line is the case of $[\mathrm{P_i}]$ equal to 1 mM, and the dashed-dot line is the case of $[\mathrm{P_i}]$ equal to 2 mM. Similarly, mechanism E is unable to reproduce the succinate-dependent inhibition of the forward reaction illustrated in Figure 4(D), where the dashed line is the case of [SUC] equal to zero, the solid line is the case of [SUC] equal to 0.5 mM and the dashed-dot line is the case of [SUC] equal to 2 mM.

To better match the experimental data and account for these phenomena, mechanism A was modified by adding dead-end binding(s) of phosphate and/or succinate to the mechanism (as

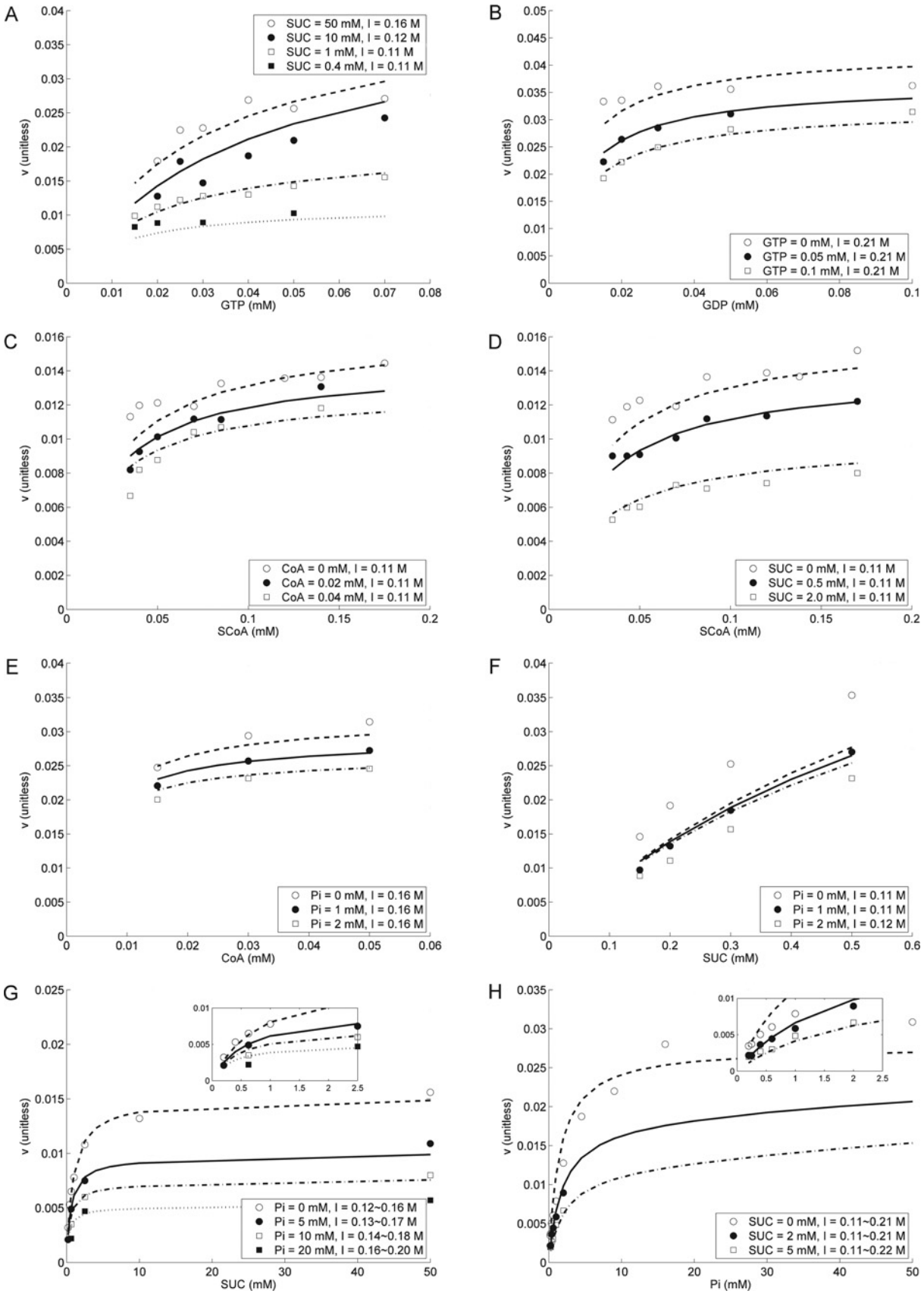

Table 3 Comparison of optimal object value and AIC number for different dead-end binding(s) of mechanisms A and E

Mechanism	Dead-end binding(s)	Optimal *M*	Total parameters	AIC
A	No	0.2552	20	45.0833
A	P_i	0.5460	21	98.943
A	SUC	0.4866	21	90.9383
A	P_i and SUC	0.1994	22	29.9353
E	No	0.2583	20	45.9225
E	SUC	0.1345	21	1.56972
E	SCoA	0.2541	21	45.7831
E	SUC and SCoA	0.1340	22	2.31087

shown in Figure 5A), and mechanism E was modified by adding dead-end binding(s) of succinate and/or succinyl-CoA to the mechanism (as shown in Figure 5B). For example, for mechanism E, trial model with dead-end succinate binding at enzyme state 2 ($E \cdot HGDP^{(2-)}$), model with dead-end binding of succinyl-CoA at enzyme state 6 ($E \cdot GTP^{(4-)}$) and model with both dead-end bindings mentioned above in the mechanism were tested against the data. Similar to Bergman et al. [28], AIC (Akaike information criterion) is used to show the trade off between goodness-of-fit and the number of parameters for this new set of candidate models

$$\mathrm{AIC} = \frac{N}{2} \ln M + n + 120 \tag{16}$$

where N is the total number of data points (which is equal to 139 here), M is the minimum normalized squared difference between model estimations and experimental data [eqn (15)], n is the total number of parameters, the constant term (120) is added to obtain positive AIC number. Smaller M means better fitting; smaller AIC means a better model. The testing results of this set of candidate models are listed in Table 3. The AIC value of mechanism E with one dead-end succinate is the minimum. Therefore it was determined that the ordered ter–ter mechanism with dead-end product inhibition of succinate against succinyl-CoA (as shown in Figure 2) is the preferred model among the candidate models.

Comparisons of the predictions of this model with the experimental data are shown in Figure 6, illustrating that it is able to simultaneously reproduce all the data of Cha and Parks. Table 4 lists estimated model parameters associated with these fits. Based on the values of rate constants listed in Table 4 and eqn (14), the calculated standard equilibrium constant K_{eq} (at $T = 303.15$ K) is 3.1390×10^{-10}. From this the standard Gibbs free energy of reaction is computed as 55.15 kJ/mol. Accounting for the experimental temperature of the Cha and Parks data [8,27] ($T = 303.15$ K) the standard Gibbs free energy of reaction at 303.15 K computed from the reported thermodynamic data in Table 1 (i.e. after temperature correction [20]) is $\Delta_r G^0 = 56.98$ kJ/mol. Thus there is a difference of 1.83 kJ/mol between the Gibbs free energy associated with the optimal kinetic parameters and the estimate reported in Li et al. [19].

Sensitivity analysis

The sensitivity of the model prediction to small changes in parameter values is investigated. By repeating the optimization with one parameter k_i^0 constrained to a value $\pm 10\%$ different from the estimated optimal value, the sensitivity of the model fit to parameter i is calculated:

$$S_i = \frac{\partial M_i(x_i)/M_i(x_i)}{\partial x_i/x_i} \approx \frac{\max\left(\left|M_i(x_i \pm 0.1x_i) - M_i(x_i)\right|\right)}{0.1M_i(x_i)} \tag{17}$$

where M is computed from eqn (15) and x_i is the value of the ith k_i^0. The sensitivity values of estimated parameters are listed in Table 4. All the estimates are larger than 1, revealing that they are all sensitive to the data. The most sensitive parameter is $k_{+6}{}^0$, with the value as large as 3.0389×10^4. Other highly sensitive parameters are $k_{-1}{}^0$, $k_{-2}{}^0$, $k_{+3}{}^0$, $k_{-3}{}^0$, $k_{+4}{}^0$, $k_{+5}{}^0$ and $k_{-5}{}^0$, with the values larger than 100.

Figure 3 Simulation results of mechanism A, partial random sequential kinetic mechanism with enzyme-bound phosphoryl CoA as an intermediate

Panels (**A**, **E** and **F**) plot data from Cha and Parks [8] and the quasi-steady reverse flux at the indicated concentration conditions. Panels (**B**, **C** and **D**) plot data from Cha and Parks [8] on the quasi-steady forward flux assayed under the indicated concentration conditions. Panel (**A**) shows data on the reverse reaction flux as a function of total GTP concentration and four different succinate concentrations, with CoA concentration held fixed at 0.1 mM. Panel (**B**) shows data on the forward reaction flux as a function of total GDP concentration and three different inhibitor GTP concentrations, with phosphate concentration held fixed at 50 mM and succinyl-CoA concentration held fixed at 0.1 mM. Panel (**C**) shows data on the forward reaction flux as a function of total succinyl-CoA concentration and three different inhibitor CoA concentrations, with phosphate concentration held fixed at 1.0 mM and GDP concentration held fixed at 0.05 mM. Panel (**D**) shows data on the forward reaction flux as a function of total succinyl-CoA concentration and three different inhibitor succinate concentrations, with phosphate concentration held fixed at 1.0 mM and GDP concentration held fixed at 0.05 mM. Panel (**E**) shows data on the reverse reaction flux as a function of total CoA concentration and three different inhibitor phosphate concentrations, with succinate concentration held fixed at 50 mM and GTP concentration held fixed at 0.1 mM. Both panels (**F**) and (**G**) show data on the reverse reaction flux as a function of total succinate concentration and different inhibitor phosphate concentrations, with CoA and GTP concentrations held fixed at 0.1 mM. Panel (**F**) shows relatively low concentrations of succinate and phosphate, while panel (**G**) shows a greater range of concentrations. Panel (**H**) shows data on the forward reaction flux as a function of total phosphate concentration and three different inhibitor succinate concentrations, with succinyl-CoA and GDP concentrations held fixed at 0.1 mM.

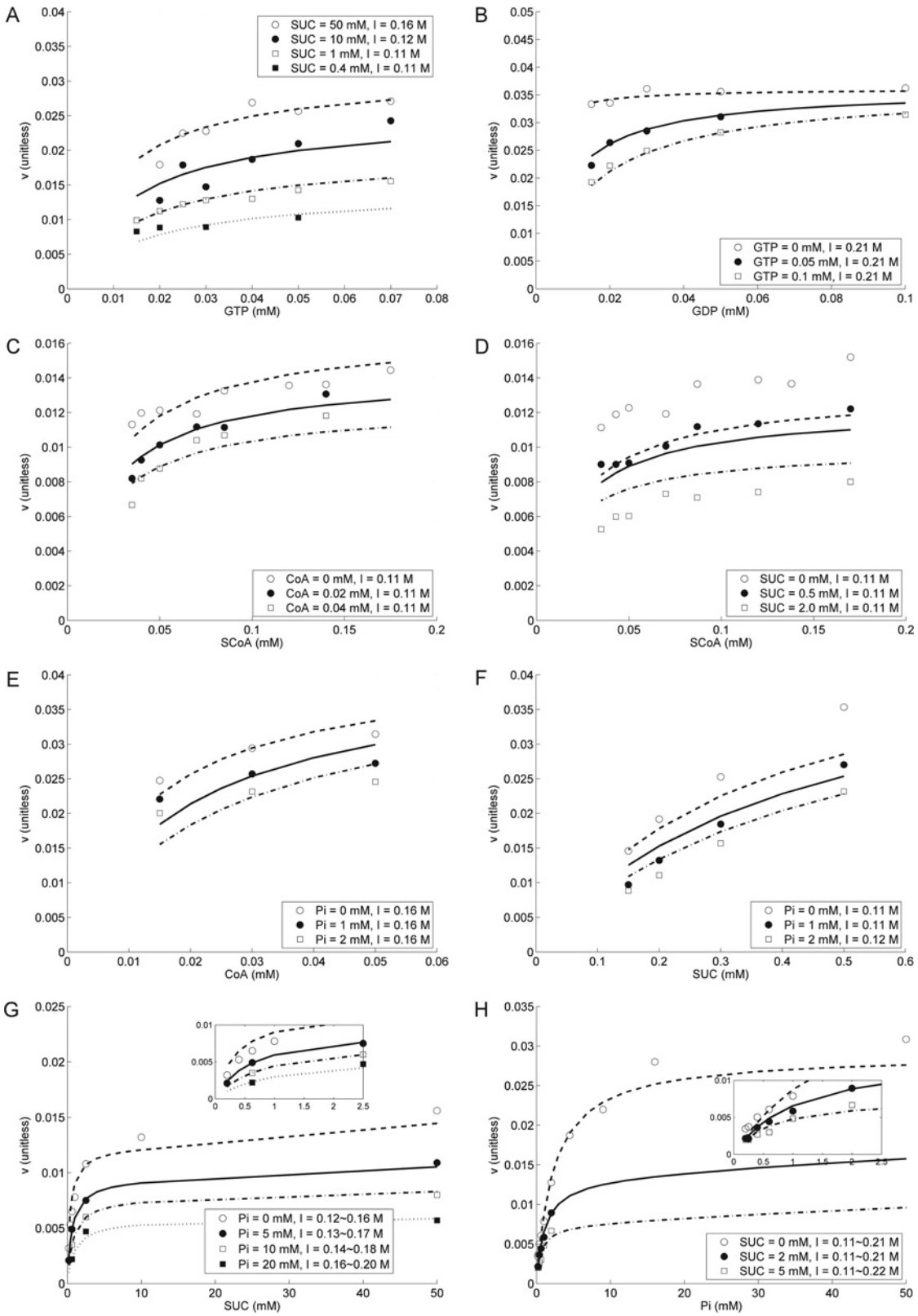

Figure 4 **Simulation results of mechanism E, ordered ter–ter kinetic mechanism**
Experimental data are same as in Figure 3.

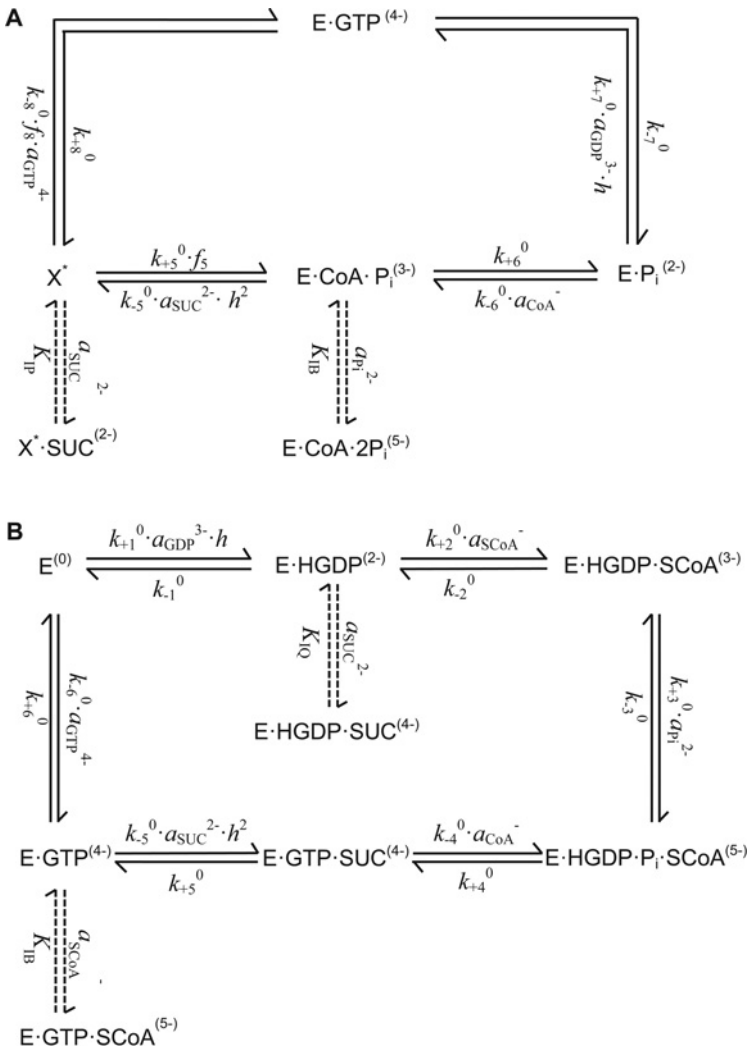

Figure 5 **Addition of dead-end binding(s) to mechanisms A and E**

(**A**) Mechanism A with dead-end binding(s) of phosphate and/or succinate. X* is the rapid equilibrium segment as shown in the Appendix. (**B**) Mechanism E with dead-end binding(s) of succinate and/or succinyl-CoA.

DISCUSSION

Discrimination of candidate kinetic models

A number of kinetic models of SCS have been proposed since the 1950s. In the present study, we examine whether these kinetic models (labelled A–E) can characterize the data of Cha and Parks on pig heart SCS with a unique set of kinetic parameters. By accounting for the effects of ionic strength on chemical species involved in fundamental kinetic steps, the optimal parameter sets are obtained for each kinetic mechanism, and corresponding simulation results are shown in Figures 3 and 4 and the Appendix. As revealed from these simulation results, mechanisms A and E exhibit significantly better agreement with the data, compared with mechanisms B, C and D.

Although mechanisms A and E represent better candidate models compared with mechanisms B, C and D, Figures 3 and 4 demonstrate their inability to fit all of the data. Inspection of Figures 3 and 4 implies the possible existence of dead-end inhibitors, for example, substrate inhibition of phosphate against succinate in mechanism A and product inhibition of succinate against succinyl-CoA in mechanism E. By systematically testing different possible dead-end bindings, dead-end product inhibition of succinate against succinyl-CoA in mechanism E is shown to significantly improve the fitting and has the minimum AIC number. Therefore the ordered ter–ter mechanism (mechanism E)

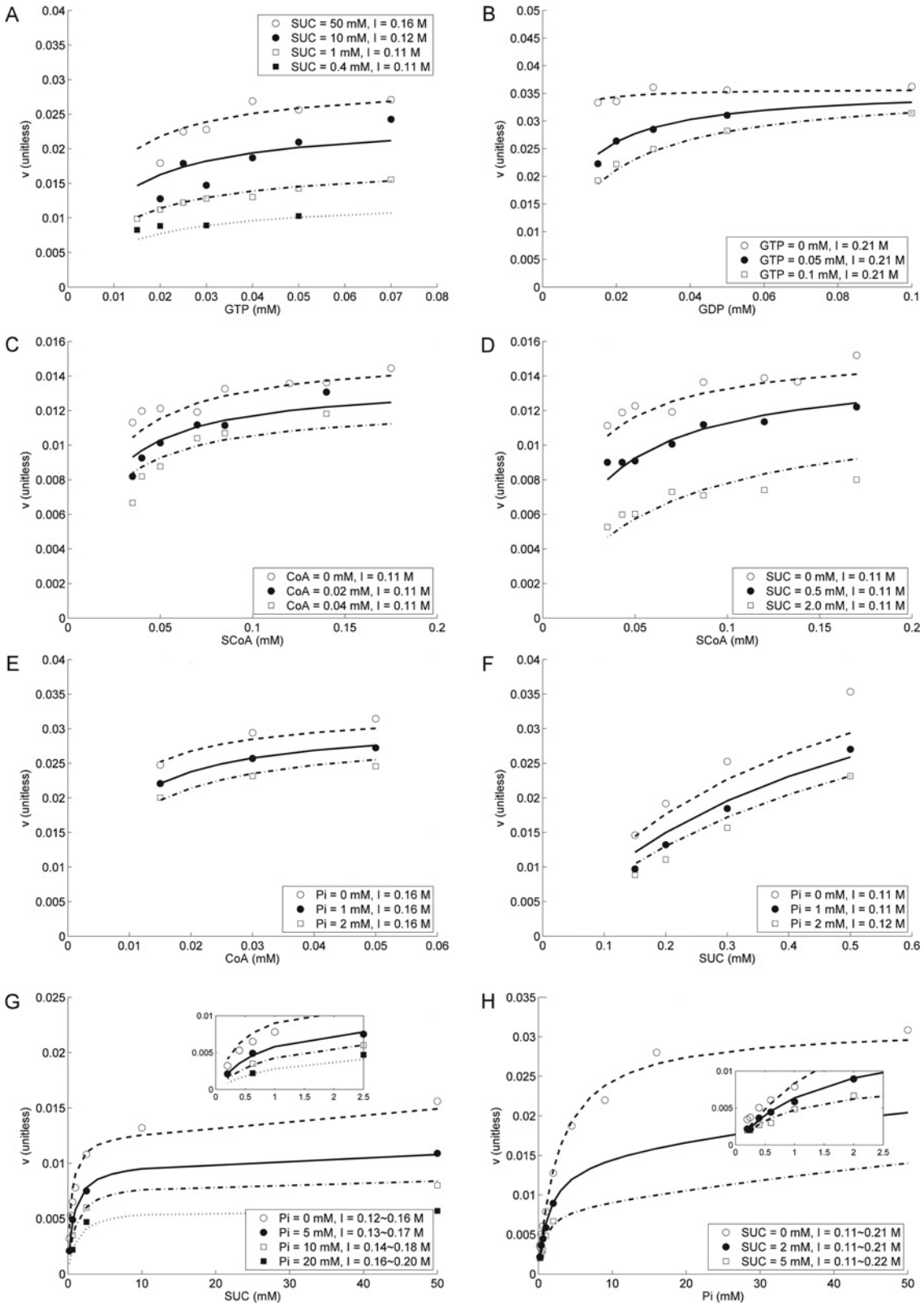

Figure 6 **Ordered ter–ter mechanism with dead-end product inhibition of succinate against succinyl-CoA**
Experimental data are the same as in Figure 3.

Table 4 Optimal object value, estimated parameters and parameter sensitivities of ordered ter–ter mechanism with dead-end product inhibition of succinate against succinyl-CoA
k_i^0 is the rate constant at $T = 303.15$ K.

Adjustable parameter	Optimum estimated value	Sensitivity	Units
Optimal M	0.1345		–
$k_{+1}{}^0$	4.6151×10^{5}	1.9040	$M^{-2}\cdot s^{-1}$
$k_{-1}{}^0$	1.6353×10^{-9}	137.3615	s^{-1}
$k_{+2}{}^0$	2.2409×10^{-5}	56.9336	$M^{-1}\cdot s^{-1}$
$k_{-2}{}^0$	8.6278×10^{-10}	2668.4195	s^{-1}
$k_{+3}{}^0$	3.1299×10^{-6}	667.7291	$M^{-1}\cdot s^{-1}$
$k_{-3}{}^0$	6.5016×10^{-7}	336.2064	s^{-1}
$k_{+4}{}^0$	1.1666×10^{-6}	240.2766	s^{-1}
$k_{-4}{}^0$	0.0295	9.6611	$M^{-1}\cdot s^{-1}$
$k_{+5}{}^0$	1.4717×10^{-7}	203.22922	s^{-1}
$k_{-5}{}^0$	5.3242×10^{10}	112.7709	$M^{-3}\cdot s^{-1}$
$k_{+6}{}^0$	6.8965×10^{-9}	3.0389×10^{4}	s^{-1}
$k_{-6}{}^0$	0.0847	1.9967	$M^{-1}\cdot s^{-1}$
$K_{I,SUC}$	1.4686×10^{-4}	22.4362	M
V_{mf} (plot A)	3.6824×10^{-2}	45.1435	$M\cdot s^{-1}$
V_{mf} (plot B)	4.0583×10^{-2}	31.8047	$M\cdot s^{-1}$
V_{mf} (plot C)	5.6983×10^{-2}	24.4405	$M\cdot s^{-1}$
V_{mf} (plot D)	5.7445×10^{-2}	24.2672	$M\cdot s^{-1}$
V_{mf} (plot E)	4.1777×10^{-2}	31.1471	$M\cdot s^{-1}$
V_{mf} (plot F)	8.6628×10^{-2}	16.9286	$M\cdot s^{-1}$
V_{mf} (plot G)	1.9710×10^{-2}	68.5088	$M\cdot s^{-1}$
V_{mf} (plot H)	3.1144×10^{-2}	31.1762	$M\cdot s^{-1}$

with dead-end product inhibition of succinate against succinyl-CoA is judged to be the optimal kinetic model that simultaneously matches the data of Cha and Parks. To our knowledge, this model represents the first thermodynamics-constrained kinetic model that is able to characterize a complete set of kinetic data of mammalian SCS.

Consideration of ionic strength effects

In this kinetic study, the effects of ionic strength effects are considered for chemical species during fundamental steps, by following the methodology previously demonstrated in Mescam et al. [18]. More traditionally such effects are ignored by treating the maximum velocities (V_m), the Michaelis (K_m) and inhibition (K_i) constants as the adjustable parameters in the model. These parameters are constrained by Haldane relationships. For example, the Haldane relationships for ordered ter–ter mechanism are:

$$K'_{eq} = \frac{K_{ip}K_{iq}K_{ir}}{K_{ia}K_{ib}K_{ic}} = \frac{V_{mf}K_{mP}K_{iq}K_{ir}}{V_{mr}K_{ia}K_{ib}K_{mC}} \qquad (18)$$

Where K'_{eq} denotes the apparent equilibrium constant, the subscript f indicates the forward reaction, r indicates the reverse reaction, a, b and c (C) denote the substrates, and p (P), q and r denote the products. In either formulation, the number of adjustable parameters in the model equals to the total number of parameters minus the number of independent Haldane relationships. The Appendix summarizes the independent Haldane relationships for each mechanism studied here. However, eqn (11) clearly shows that the Michaelis (K_m) and inhibition (K_i) are functions of temperature and ionic strength, which means that they have different values under different temperatures and ionic strength conditions. Our strategy uses rate constants as parameters, which may be estimated by the Arrhenius relation as functions of temperature only. Furthermore, our strategy implicitly accounts for the relationship between reaction equilibrium constant and rate constants.

Other candidate model

Previous studies of *E. coli* SCS revealed the existence of phosphoenzyme ($E\cdot P_i$) [1,29,30] and enzyme-bound succinyl phosphate ($E\cdot$Succinyl-P_i) [12] as enzyme intermediates. Since a previous structure study of pig heart GTP-specific SCS also supported that the dephosphorylated structure of the enzyme can be stabilized by the binding of a phosphate ion [24], we assumed that phosphoenzyme and enzyme-bound succinyl phosphate are also enzyme intermediates in pig heart SCS and evaluated the mechanism, as shown in Figure A6 of the Appendix. This mechanism accounts for two enzyme subunits, labelled α and β. In this mechanism, phosphate ion binds to the α subunit to stabilize the enzyme, forming the intermediate phosphoenzyme. Subsequently, succinyl-CoA is added and CoA is released to form the intermediate enzyme-bound succinyl phosphate. After succinate is released, GDP binds to (the N-terminal domain of) the β subunit, and the active-site histidine residue swings to the GDP-binding site to shuttle the phosphoryl group [31]. Finally, GTP forms then releases from the enzyme. This mechanism can be simplifies to a Bi–Bi–Uni–Uni ter–ter kinetic mechanism (Figure A7). However, simulations of this model are not consistent with the Cha and Parks' data (as shown in Figure A8), indicating that the assumption of phosphoenzyme and enzyme-bound succinyl phosphate as intermediates in pig heart SCS cannot explain the data. Therefore this proposed mechanism is excluded.

Roles of inorganic phosphate in regulating SCS reverse flux

Cha and Parks [8] found that the initial reaction velocity of the reverse reaction decreased with increasing concentration of the product inorganic phosphate. However, a conflicting result was reported by Phillips et al. [32], who proposed that SCS is activated by increasing phosphate concentration. Since the Cha and Parks' data conflict with the data of Phillips et al., both datasets cannot be resolved in a single model. Further experiments are required to elucidate the possible effect of phosphate on the reverse flux of SCS.

Conclusions

In the present study, in order to account for the effects of ionic strength on the kinetics of pig heart SCS, each enzyme–substrate complex is assigned by an effective charge for each fundamental step, and rate constants are as parameters to integrate modelling. The ordered ter–ter mechanism with dead-end product inhibition of succinate against succinyl-CoA is shown to effectively match kinetic data on pig heart SCS. To our knowledge, this model represents the first thermodynamic-constrained kinetic model that is able to characterize a complete set of kinetic data of mammalian SCS. However, conflicted findings exist for the roles of inorganic phosphate in regulating SCS reverse flux. Further experiments are required to probe the possible effect of phosphate on the reverse flux of SCS.

APPENDIX

Rate equation derivation of mechanisms A and D

Substrates are designated by the letters A, B and C in the order of adding to the enzyme, and products are denoted by the letters P, Q and R in the order of leaving the enzyme. Comparing mechanism A with mechanism D, the difference is the sequence of products P and Q. That means that the basic figure of mechanisms A and D is the same, as shown in Figure A1.

According to the method presented by Cleland [25] to write the rate equation in coefficient form, there are in total 52 terms in the denominator of the rate equation (of mechanisms A and D) and 16 square terms among them. Then rapid equilibrium assumption is applied to simplify the rate equation. By assuming that the dissociations of EA, EB and EAB in Figure A1 are very rapid compared with the rates of the forward steps, and

$$K_A = \frac{k_{-1}}{k_{+1}} = \frac{k_{-4}}{k_{+4}} = \frac{[E][A]}{[EA]} = \frac{[EB][A]}{[EAB]},$$
$$K_B = \frac{k_{-2}}{k_{+2}} = \frac{k_{-3}}{k_{+3}} = \frac{[E][B]}{[EB]} = \frac{[EA][B]}{[EAB]} \quad \text{(A1)}$$

we can assign

$$[X] = [E] + [EA] + [EB] + [EAB] \quad \text{(A2)}$$

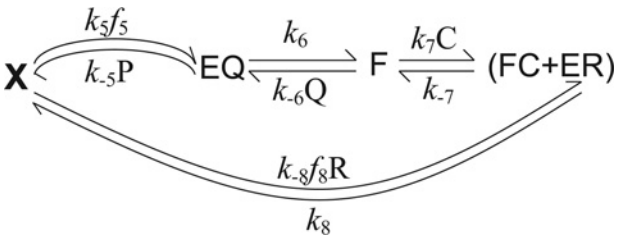

Figure A2 Basic figure of mechanisms A and D with rapid equilibrium segment

f_5 and f_8 is the fraction of [EAB] and [E] in [X] respectively.

which represents the rapid equilibrium segment.

Then, the basic figure can be condensed to Figure A2. From eqn (A1), [EA], [EB] and [EAB] can be expressed as functions of [E]:

$$[EA] = \frac{[A]}{K_4}[E],$$
$$[EB] = \frac{[B]}{K_B}[E],$$
$$[EAB] = \frac{[A][B]}{K_A K_B}[E] \quad \text{(A3)}$$

Combining eqns (A1)–(A3), the fraction of [EAB] and [E] in [X], which denotes f_5 and f_8 respectively, can be calculated:

$$f_5 = \frac{[A][B]}{K_A K_B + K_B[A] + K_A[B] + [A][B]},$$
$$f_8 = \frac{K_A K_B}{K_A K_B + K_B[A] + K_A[B] + [A][B]} \quad \text{(A4)}$$

The rate equation can be expressed as $v = k_{+5} f_5[X] - k_{-5}[P][EQ]$. Using this expression to rewrite the rate equation in coefficient form, as shown in equation (A5), there are only 20 terms in the denominator and all the squared concentration terms

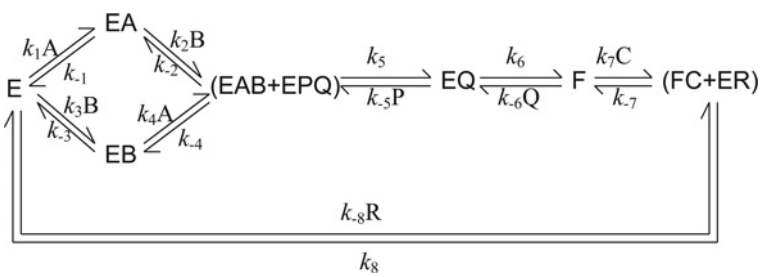

Figure A1 The basic figure of mechanisms A and D

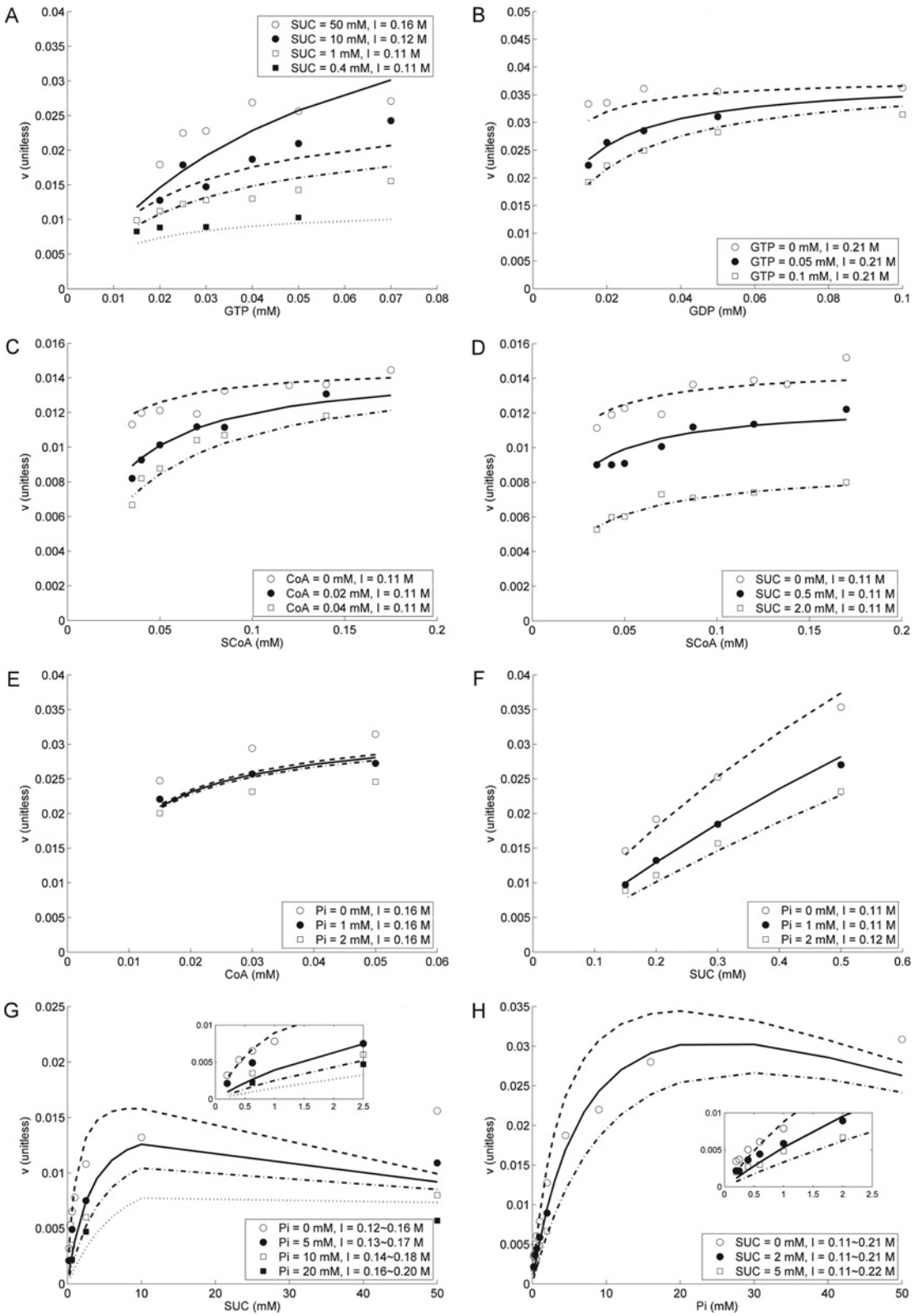

Figure A3 Simulation results of mechanism B, complicated fully random with dead-end complexes kinetic mechanism [8]

Experimental data are the same as in Figure 3.

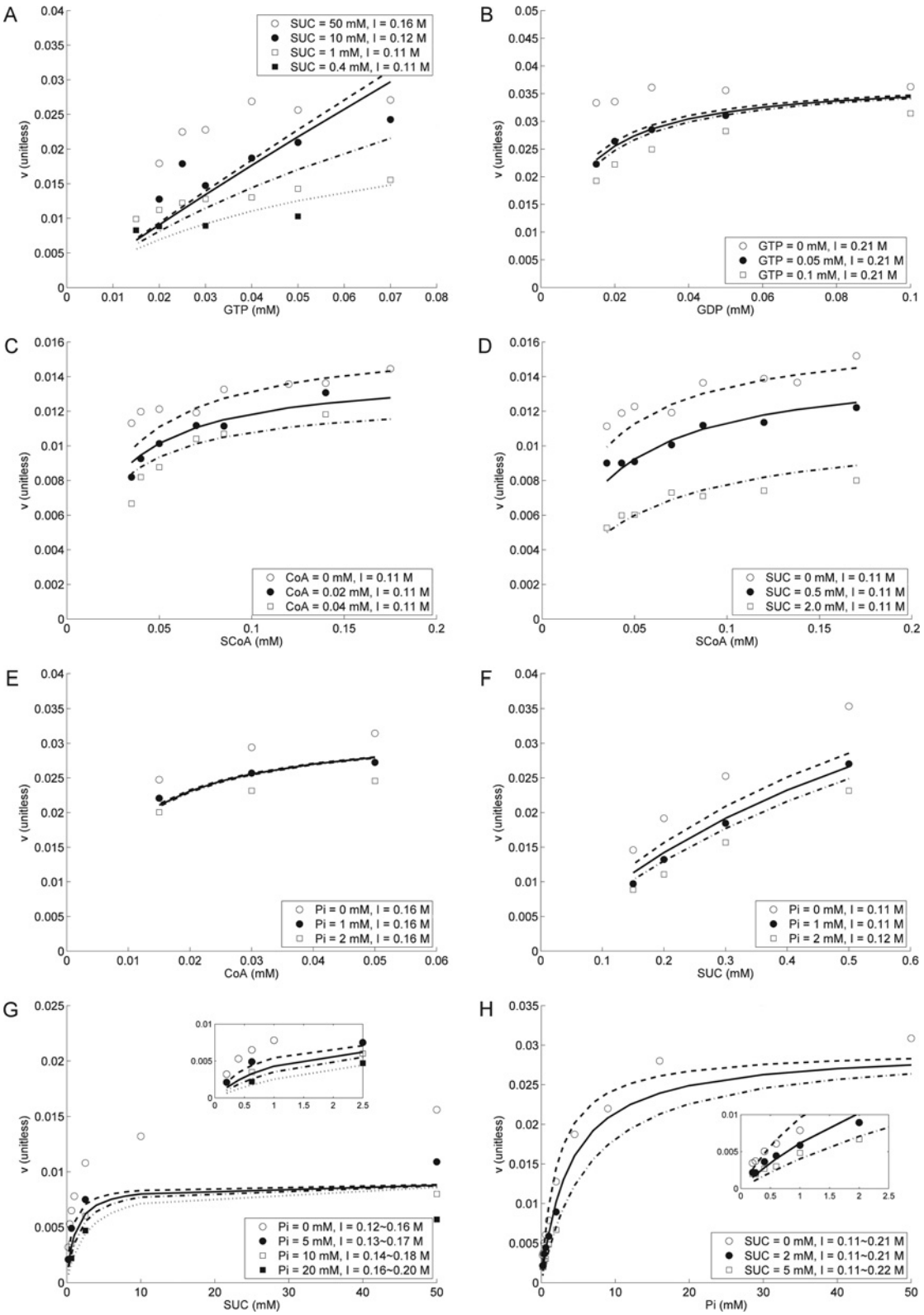

Figure A4 Simulation results of mechanism C, Hexa-Uni Ping Pong ter–ter mechanism with high-energy enzyme-bound CoA as an intermediate [9,10]

Experimental data are the same as in Figure 3.

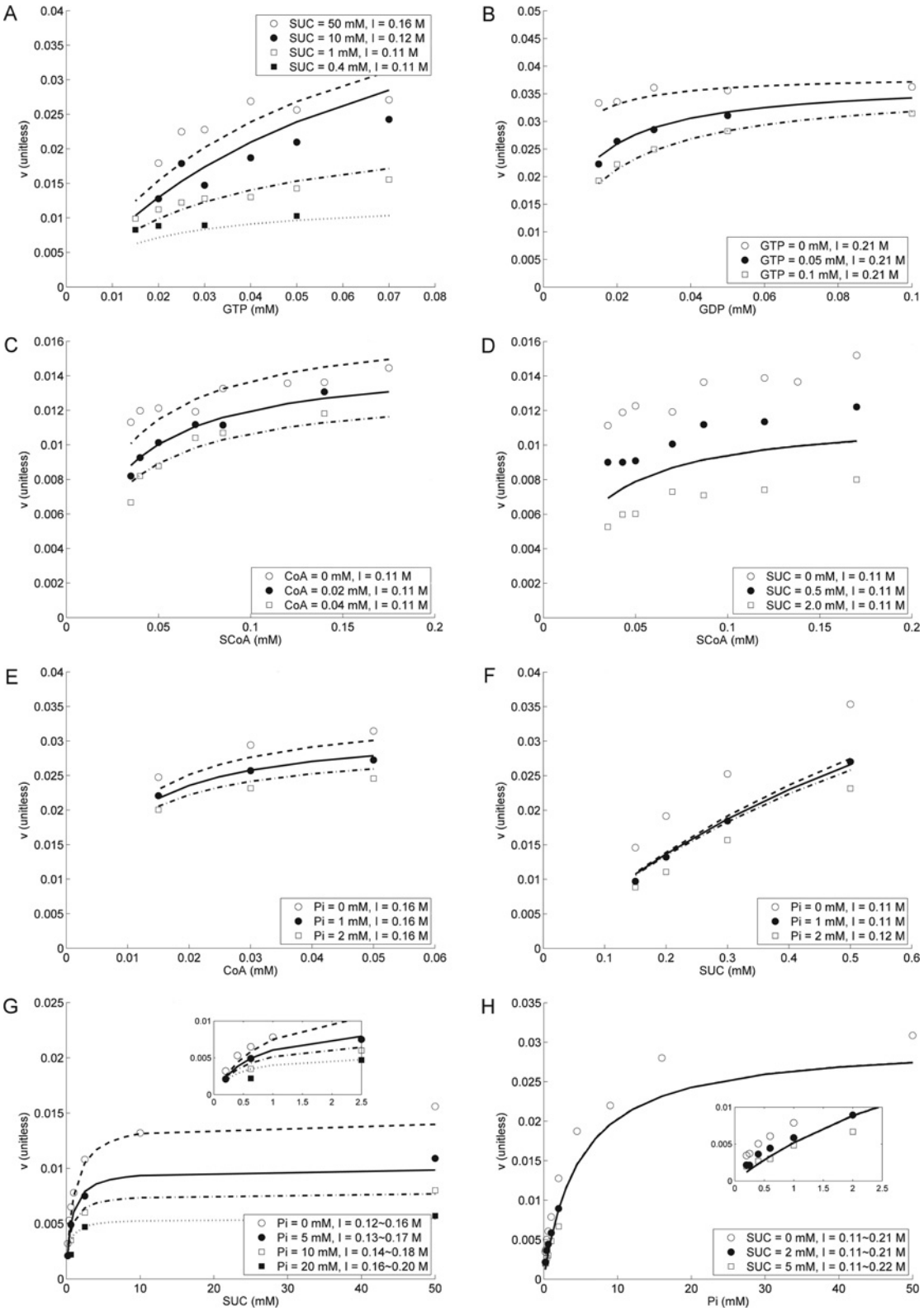

Figure A5 Simulation results of mechanism D, partial random sequential kinetic mechanism with enzyme-bound succinyl phosphate as an intermediate [12]

Experimental data are the same as in Figure 3.

are eliminated by rapid equilibrium assumption.

$$v = \frac{V_{mf}V_{mr}([A][B][C] - \frac{[P][Q][R]}{K_{eq}})}{V_{mr}K_{mA}K_{ib}[C] + \frac{V_{mr}K_{mA}K_{ib}K_{ic}[R]}{K_{ir}} + V_{mr}K_{mC}[A][B] + V_{mr}K_{mB}[A][C] + V_{mr}K_{mA}[B][C]}$$
$$+\frac{V_{mr}K_{mA}K_{ib}K_{mQ}[C][P]}{K_{mP}K_{iq}} + \frac{V_{mr}K_{mA}K_{ib}[C][R]}{K_{ir}} + \frac{V_{mf}K_{mR}[P][Q]}{K_{eq}} + \frac{V_{mf}K_{mQ}[P][R]}{K_{eq}} + \frac{V_{mf}K_{mP}[Q][R]}{K_{eq}}$$
$$+V_{mr}[A][B][C] + \frac{V_{mf}K_{mR}K_{ip}[A][B][Q]}{K_{ia}K_{ib}K_{eq}} + \frac{V_{mf}K_{mQ}K_{ir}[A][C][P]}{K_{ia}K_{ic}K_{eq}} + \frac{V_{mf}K_{mR}[A][P][Q]}{K_{ia}K_{eq}}$$
$$+\frac{V_{mf}K_{mQ}K_{ir}[B][C][P]}{K_{ib}K_{ic}K_{eq}} + \frac{V_{mf}K_{mR}[B][P][Q]}{K_{ib}K_{eq}} + \frac{V_{mf}K_{mQ}[C][P][R]}{K_{ic}K_{eq}} + \frac{V_{mf}[P][Q][R]}{K_{eq}}$$
$$+\frac{V_{mf}K_{mQ}K_{ir}[A][B][C][P]}{K_{ia}K_{ib}K_{ic}K_{eq}} + \frac{V_{mf}K_{mR}[A][B][P][Q]}{K_{ia}K_{ib}K_{eq}} \quad \text{(A5)}$$

where

$$K_{mA} = \frac{Coef_{BC}}{Coef_{ABC}} = K_A \cdot \frac{k_{+6}k_{+8}}{(k_{+5}k_{+6} + k_{+5}k_{+8} + k_{+6}k_{+8})},$$
$$K_{mB} = \frac{Coef_{AC}}{Coef_{ABC}} = K_B \cdot \frac{k_{+6}k_{+8}}{(k_{+5}k_{+6} + k_{+5}k_{+8} + k_{+6}k_{+8})},$$
$$K_{mC} = \frac{Coef_{AB}}{Coef_{ABC}} = \frac{k_{+5}k_{+6}(k_{-7} + k_{+8})}{k_{+7}(k_{+5}k_{+6} + k_{+5}k_{+8} + k_{+6}k_{+8})},$$
$$K_{mP} = \frac{Coef_{QR}}{Coef_{PQR}} = \frac{k_{-7}}{k_{-5}},$$
$$K_{mQ} = \frac{Coef_{PR}}{Coef_{PQR}} = \frac{k_{-7}}{k_{-6}},$$
$$K_{mR} = \frac{Coef_{PQ}}{Coef_{PQR}} = \frac{k_{-7} + k_8}{k_{-8}},$$
$$K_{ia} = \frac{Coef_C}{Coef_{AC}} = \frac{Coef_{CP}}{Coef_{ACP}} = \frac{Coef_{PQ}}{Coef_{APQ}} = \frac{Coef_{BCP}}{Coef_{ABCP}} = \frac{Coef_{BPQ}}{Coef_{ABPQ}} = \frac{k_{-1}}{k_{+1}} = K_A,$$
$$K_{ib} = \frac{Coef_C}{Coef_{BC}} = \frac{Coef_{CP}}{Coef_{BCP}} = \frac{Coef_{PQ}}{Coef_{BPQ}} = \frac{Coef_{ACP}}{Coef_{ABCP}} = \frac{Coef_{APQ}}{Coef_{ABPQ}} = \frac{k_{-2}}{k_{+2}} = K_B,$$
$$K_{ic} = \frac{Coef_R}{Coef_{CR}} = \frac{Coef_{PR}}{Coef_{CPR}} = \frac{k_{-7}}{k_{+7}},$$
$$K_{ip} = \frac{Coef_{ABQ}}{Coef_{ABPQ}} = \frac{k_{+5}}{k_{-5}},$$
$$K_{iq} = \frac{Coef_R}{Coef_{QR}} = \frac{Coef_{AB}}{Coef_{ABQ}} = \frac{k_{+6}}{k_{-6}},$$
$$K_{ir} = \frac{Coef_C}{Coef_{CR}} = \frac{Coef_{CP}}{Coef_{CPR}} = \frac{k_{+8}}{k_{-8}},$$
$$V_{mf} = [E]_t \frac{k_{+5}k_{+6}k_{+8}}{k_{+5}k_{+6} + k_{+5}k_{+8} + k_{+6}k_{+8}},$$
$$V_{mr} = [E]_t k_{-7} \quad \text{(A6)}$$

And, Haldane relationships are:

$$K_{eq} = \frac{K_{ip}K_{iq}K_{ir}}{K_{ia}K_{ib}K_{ic}} = \frac{V_{mf}K_{mP}K_{iq}K_{ir}}{V_{mr}K_{mA}K_{ib}K_{ic}} = \frac{V_{mf}K_{mP}K_{iq}K_{ir}}{V_{mr}K_{mB}K_{ia}K_{ic}} = \frac{V_{mf}K_{mR}K_{ip}K_{iq}}{V_{mr}K_{mC}K_{ia}K_{ib}} \quad \text{(A7)}$$

Simulation results of models B, C and D with chemical species activities

Simulation results of models B, C and D with chemical species activities are shown in Figures A3–A5 respectively. Plots (A)–(G) correspond to Figures 5–12 respectively in Cha and Parks' paper [8]. The simulation results are shown as lines, and experimental data are shown as points.

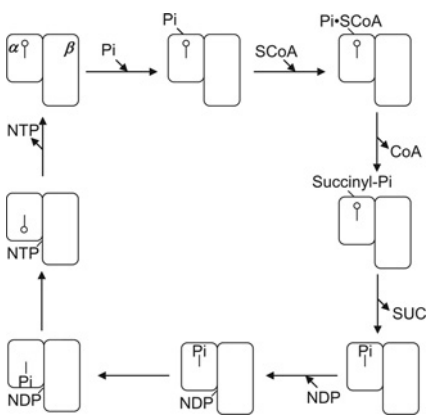

Figure A6 An alternative mechanism proposed for pig heart GTP-specific SCS

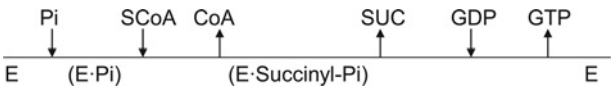

Figure A7 Bi–Bi–Uni–Uni ter–ter kinetic mechanism

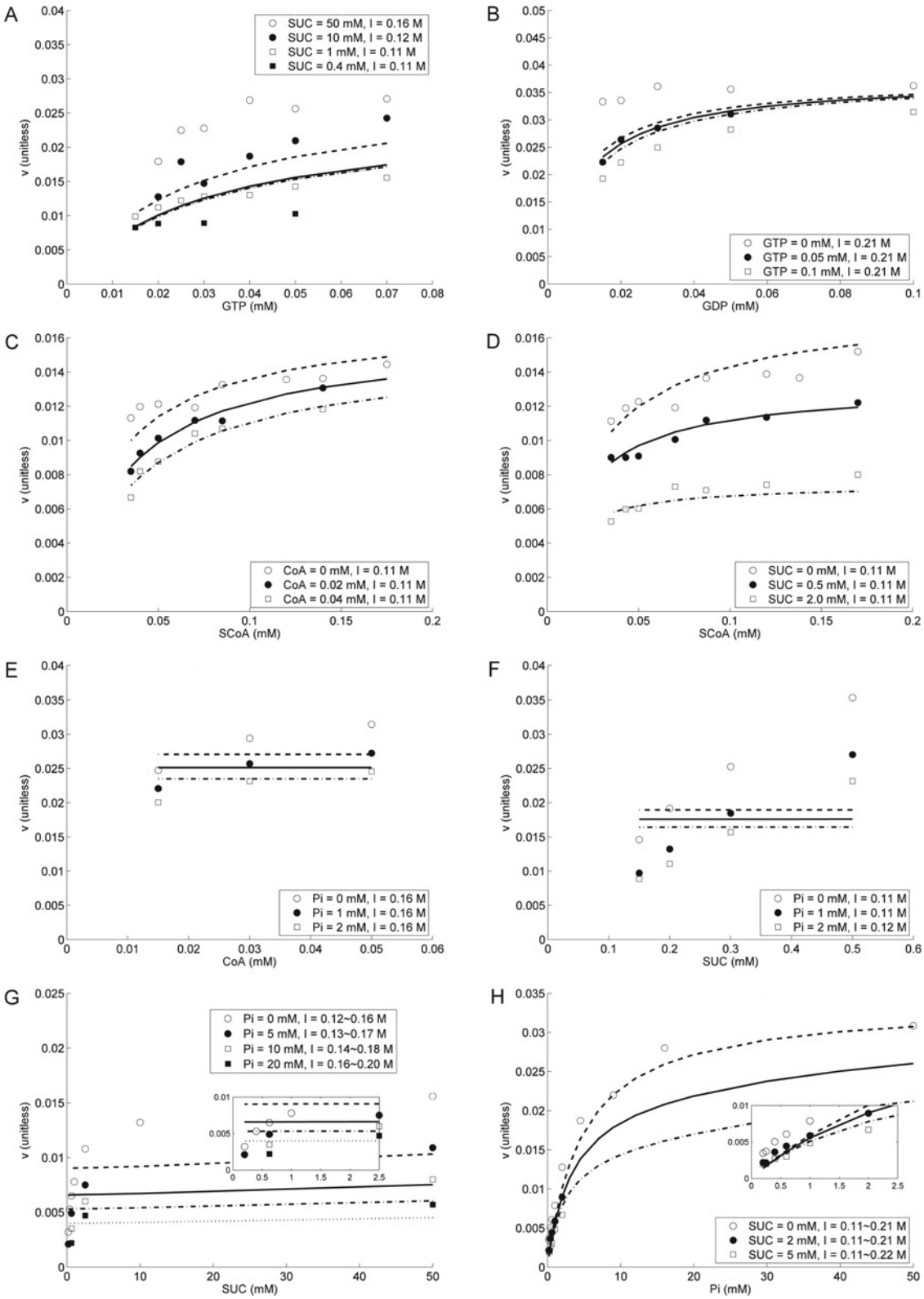

Figure A8 Simulation results of proposed Bi–Bi–Uni–Uni ter–ter mechanism

Plots (A)–(G) correspond to Figures 5–12 respectively in Cha and Parks [8]. The simulation results are shown as lines, and experimental data are shown as points. Experimental data are the same as in Figure 3.

Independent Haldane relationships for each mechanism

Mechanism	Independent Haldane relationships
A	$K_{eq} = \frac{K_{ip}K_{iq}K_{ir}}{K_{ia}K_{ib}K_{ic}} = \frac{V_{mf}K_{mP}K_{iq}K_{ir}}{V_{mr}K_{mA}K_{ib}K_{ic}} = \frac{V_{mf}K_{mP}K_{iq}K_{ir}}{V_{mr}K_{mB}K_{ia}K_{ic}} = \frac{V_{mf}K_{mR}K_{ip}K_{iq}}{V_{mr}K_{mC}K_{ia}K_{ib}}$
B	$K_{eq} = \frac{K_{ip}K_{mQ}K_{ir}}{K_{ia}K_{mB}K_{ic}} = \frac{V_{mf}K_{mQ}K_{ip}K_{ir}}{V_{mr}K_{mB}K_{mC}K_{ia}} = \frac{V_{mf}K_{mQ}K_{ip}K_{ir}}{V_{mr}K_{mA}K_{mC}K_{ib}} = \frac{V_{mf}K_{mR}K_{ip}K_{iq}}{V_{mr}K_{mB}K_{mC}K_{ia}} = \frac{V_{mf}K_{mP}K_{mQ}K_{ir}}{V_{mr}K_{mA}K_{ib}K_{ic}}$
C	$K_{eq} = \frac{K_{ip}K_{iq}K_{ir}}{K_{ia}K_{ib}K_{ic}} = \frac{V_{mf}K_{mP}K_{iq}K_{ir}}{V_{mr}K_{mA}K_{ib}K_{ic}} = \frac{V_{mf}K_{mQ}K_{ip}K_{ir}}{V_{mr}K_{mB}K_{ia}K_{ic}} = \frac{V_{mf}K_{mR}K_{ip}K_{iq}}{V_{mr}K_{mC}K_{ia}K_{ib}}$
D	$K_{eq} = \frac{K_{ip}K_{iq}K_{ir}}{K_{ia}K_{ib}K_{ic}} = \frac{V_{mf}K_{mP}K_{iq}K_{ir}}{V_{mr}K_{mA}K_{ib}K_{ic}} = \frac{V_{mf}K_{mP}K_{iq}K_{ir}}{V_{mr}K_{mB}K_{ia}K_{ic}} = \frac{V_{mf}K_{mR}K_{ip}K_{iq}}{V_{mr}K_{mC}K_{ia}K_{ib}}$
E	$K_{eq} = \frac{K_{ip}K_{iq}K_{ir}}{K_{ia}K_{ib}K_{ic}} = \frac{V_{mf}K_{mP}K_{iq}K_{ir}}{V_{mr}K_{ia}K_{ib}K_{mC}}$

Alternative mechanism for pig heart GTP-specific SCS

An alternative mechanism proposed for pig heart GTP-specific SCS is shown in Figure A6: the smaller box denotes α-subunit, and the bigger one is β-subunit. Phosphate binds to α-subunit first to stabilize the enzyme. Then succinyl-CoA is added and CoA is released to form the intermediate enzyme-bound succinyl phosphate. After succinate is released, GDP binds to (the N-terminal domain of) the β-subunit, and the active-site histidine residue swings to the GDP-binding site to shuttle the phosphoryl group. At last, GTP forms then releases from the enzyme.

Nomenclature

a, activity; B, an empirical constant taken to be 1.6 $M^{-1/2}$; c, species concentration; $\Delta_r G^0$, standard Gibbs free energy of reaction; h, hydrogen ion activity; I, ionic strength; $J_{i,j}^{sim}$, the simulated flux; $J_{i,j}^{exp}$, the experimental flux; K, dissociation constant; K_{eq}, chemical (reference reaction) equilibrium constant; K'_{eq}, apparent equilibrium constant; K_i, inhibition constant; K_m, Michaelis constant; k_i^0, rate constant; M, minimum normalized squared difference between model estimations and experimental data; N, total data points; n, total parameter numbers; P_j, binding polynomial associated with reactant j; R, gas constant (8.3145 $J \cdot K^{-1} \cdot mol^{-1}$); S, sensitivity; T, temperature; V_{mf}, forward maximum velocity; V_{mr}, backward maximum velocity; γ, activity coefficient; z, valence of species.

AUTHOR CONTRIBUTION

Xin Li conceived, designed and carried out the study, with help from Fan Wu and Daniel Beard. Xin Li wrote the paper, with help from Fan Wu and Daniel Beard.

FUNDING

This work was supported by the National Institutes of Health (NIH) [grant numbers R01-HL072011, P50-GM094503].

REFERENCES

1 Bridger, W. A. (1974) Succinyl-CoA synthetase. In The Enzymes (Boyer, P. D., ed.), pp. 581–606, Academic Press, London/New York

2 Joyce, M. A. (2000) Structural and Functional Studies of Succinyl-CoA Synthetase. Ph. D. Thesis University of Alberta, Edmonton, AB, Canada

3 Labbe, R. F., Kurumada, T. and Onisawa, J. (1965) The role of succinyl-CoA synthetase in the control of heme biosynthesis. Biochim. Biophys. Acta **111**, 403–415

4 Alarcon, C., Wicksteed, B., Prentki, M., Corkey, B. E. and Rhodes, C. J. (2002) Succinate is a preferential metabolic stimulus-coupling signal for glucose-induced proinsulin biosynthesis translation. Diabetes **51**, 2496–2504

5 Fahien, L. A. and MacDonald, M. J. (2002) The succinate mechanism of insulin release. Diabetes **51**, 2669–2676

6 Brière, J. J., Favier, J., Gimenez-Roqueplo, A. P. and Rustin, P. (2006) Tricarboxylic acid cycle dysfunction as a cause of human diseases and tumor formation. Am. J. Physiol. Cell Physiol. **291**, C1114–C1120

7 Kaufman, S. (1955) Studies on the mechanism of the reaction catalyzed by the phosphorylating enzyme. J. Biol. Chem. **216**, 153–164

8 Cha, S. and Parks, Jr, R. E. (1964) Succinic thiokinase. II. Kinetic studies: initial velocity, product inhibition, and effect of arsenate. J. Biol. Chem. **239**, 1968–1977

9 Cha, S., Cha, C. J. and Parks, Jr, R. E. (1965) Succinic thiokinase. 3. The occurrence of a nonphosphorylated high energy intermediate of the enzyme. J. Biol. Chem. **240**, 3700–3702

10 Moyer, R. W., Ramaley, R. F., Butler, L. G. and Boyer, P. D. (1967) The formation and reactions of a nonphosphorylated high energy form of succinyl coenzyme A synthetase. J. Biol. Chem. **242**, 4299–4309

11 Hager, L. P. (1962) Succinyl CoA synthetase. In The Enzymes (Boyer, P. D., Lardy, H. and Myrback, K., eds), pp. 387–394, Academic Press, London/New York

12 Nishimura, J. S. (1986) Succinyl-CoA synthetase structure-function relationships and other considerations. Adv. Enzymol. Relat. Areas Mol. Biol. **58**, 141–172

13 Nishimura, J. S., Manning, J. M. and Meister, A. (1962) Studies on the mechanism of activation acid beta-decarboxylase by alpha-keto acids and pyridoxal 5′-phosphate. Biochemistry **1**, 442–447

14 Kohn, M. C., Achs, M. J. and Garfinkel, D. (1979) Computer simulation of metabolism in pyruvate-perfused rat heart. II. Krebs cycle. Am. J. Physiol. Regul. Integr. Comp. Physiol. **237**, R159–R166

15 Moffet, F. J. and Bridger, W. A. (1973) Succinyl coenzyme A synthetase of *Escherichia coli*: initial rate kinetics of succinyl-CoA cleavage and isotope exchange studies. Can. J. Biochem. **51**, 44–55

16 Moffet, R. J. and Bridger, W. A. (1970) The kinetics of succinyl coenzyme A synthetase from *Escherichia coli*. A reaction with a covalent enzyme-substrate intermediate not exhibiting 'ping-pong' kinetics. J. Biol. Chem. **245**, 2758–2762

17 Beard, D. A., Vinnakota, K. C. and Wu, F. (2008) Detailed enzyme kinetics in terms of biochemical species: study of citrate synthase. PLoS ONE **3**, e1825

18 Mescam, M., Vinnakota, K. C. and Beard, D. A. (2011) Identification of the catalytic mechanism and estimation of kinetic parameters for fumarase. J. Biol. Chem. **286**, 21100–21109

19 Li, X., Wu, F., Qi, F. and Beard, D. A. (2011) A database of thermodynamic properties of the reactions of glycolysis, the tricarboxylic acid cycle, and the pentose phosphate pathway. Database (Oxford) **2011**, bar005

20 Li, X., Dash, R. K., Pradhan, R. K., Qi, F., Thompson, M., Vinnakota, K. C., Wu, F., Yang, F. and Beard, D. A. (2010) A database of thermodynamic quantities for the reactions of glycolysis and the tricarboxylic acid cycle. J. Phys. Chem. B **114**, 16068–16082
21 Beard, D. A. and Qian, H. (2008) Conventions and calculations for biochemical systems. In Chemical Biophysics: Quantitative Analysis of Cellular Systems, pp. 24–40, Cambridge University Press, Cambridge
22 Alberty, R. A. (2003) Thermodynamics of Biochemical Reactions, Wiley-Interscience, Hoboken
23 Johnson, J. D., Mehus, J. G., Tews, K., Milavetz, B. I. and Lambeth, D. O. (1998) Genetic evidence for the expression of ATP- and GTP-specific succinyl-CoA synthetases in multicellular eucaryotes. J. Biol. Chem. **273**, 27580–27586
24 Fraser, M. E., James, M. N., Bridger, W. A. and Wolodko, W. T. (2000) Phosphorylated and dephosphorylated structures of pig heart, GTP-specific succinyl-CoA synthetase. J. Mol. Biol. **299**, 1325–1339
25 Cleland, W. W. (1963) The kinetics of enzyme-catalyzed reactions with two or more substrates or products. I. Nomenclature and rate equations. Biochim. Biophys. Acta **67**, 104–137
26 Segel, I. H. (1993) Enzyme Kinetics, Wiley Classics Library edition, Wiley Interscience, New York
27 Cha, S. and Parks, Jr, R. E. (1964) Succinic thiokinase. I. Purification of the enzyme from pig heart. J. Biol. Chem. **239**, 1961–1967
28 Bergman, R. N., Ider, Y. Z., Bowden, C. R. and Cobelli, C. (1979) Quantitative estimation of insulin sensitivity. Am. J. Physiol. **236**, E667–E677
29 Bridger, W. A., Millen, W. A. and Boyer, P. D. (1968) Substrate synergism and phosphoenzyme formation in catalysis by succinyl coenzyme A synthetase. Biochemistry **7**, 3608–3616
30 Grinnell, F. and Nishimura, J. S. (1969) Studies on the catalytic mechanism of *Escherichia coli* succinic thiokinase. Biochemistry **8**, 4126–4130
31 Fraser, M. E., James, M. N., Bridger, W. A. and Wolodko, W. T. (1999) A detailed structural description of *Escherichia coli* succinyl-CoA synthetase. J. Mol. Biol. **285**, 1633–1653
32 Phillips, D., Aponte, A. M., French, S. A., Chess, D. J. and Balaban, R. S. (2009) Succinyl-CoA synthetase is a phosphate target for the activation of mitochondrial metabolism. Biochemistry **48**, 7140–7149

Received 23 July 2012/28 August 2012; accepted 17 September 2012

Published as Immediate Publication 23 October 2012, doi 10.1042/BSR20120069